THE STEIN PARTICLE DETECTOR

John Glen Sample

Regents of the University of California
The University of California, Berkeley
2150 Shattuck Ave, RM 313
Berkeley, CA 94704-5940

27 February 2015

Final Report

AIR FORCE RESEARCH LABORATORY
Space Vehicles Directorate
3550 Aberdeen Ave SE
AIR FORCE MATERIEL COMMAND
KIRTLAND AIR FORCE BASE, NM 87117-5776

DTIC COPY

NOTICE AND SIGNATURE PAGE

Using Government drawings, specifications, or other data included in this document for any purpose other than Government procurement does not in any way obligate the U.S. Government. The fact that the Government formulated or supplied the drawings, specifications, or other data does not license the holder or any other person or corporation; or convey any rights or permission to manufacture, use, or sell any patented invention that may relate to them.

This report was cleared for public release by the 377 ABW Public Affairs Office and is available to the general public, including foreign nationals. Copies may be obtained from the Defense Technical Information Center (DTIC) (http://www.dtic.mil).

AFRL-RV-PS-TR-2015-0094 HAS BEEN REVIEWED AND IS APPROVED FOR PUBLICATION IN ACCORDANCE WITH ASSIGNED DISTRIBUTION STATEMENT.

//SIGNED//   //SIGNED//

_____   _____
Adrian Wheelock   Glenn M. Vaughan, Colonel, USAF
Project Manager, AFRL/RVBXR   Chief, Battlespace Environment Division

This report is published in the interest of scientific and technical information exchange, and its publication does not constitute the Government's approval or disapproval of its ideas or findings.

REPORT DOCUMENTATION PAGE

Form Approved
OMB No. 0704-0188

1. REPORT DATE *(DD-MM-YYYY)* 27-02-2015	2. REPORT TYPE Final Report	3. DATES COVERED *(From - To)* 24 Nov 2010 to 31 Jan 2015
4. TITLE AND SUBTITLE The STEIN Particle Detector		5a. CONTRACT NUMBER FA9453-11-C-0008
		5b. GRANT NUMBER
		5c. PROGRAM ELEMENT NUMBER 62601F
6. AUTHOR(S) John Glen Sample		5d. PROJECT NUMBER 1010
		5e. TASK NUMBER PPM00010548
		5f. WORK UNIT NUMBER EF004516
7. PERFORMING ORGANIZATION NAME(S) AND ADDRESS(ES) Regents of the University of California The University of California, Berkeley 2150 Shattuck Ave, RM 313 Berkeley, CA 94704-5940		8. PERFORMING ORGANIZATION REPORT NUMBER
9. SPONSORING / MONITORING AGENCY NAME(S) AND ADDRESS(ES) Air Force Research Laboratory Space Vehicles Directorate 3550 Aberdeen Ave SE Kirtland AFB, NM 87117-5776		10. SPONSOR/MONITOR'S ACRONYM(S) AFRL/RVBX
		11. SPONSOR/MONITOR'S REPORT NUMBER(S) AFRL-RV-PS-TR-2015-0094

12. DISTRIBUTION / AVAILABILITY STATEMENT

Approved for Public Release; distribution is unlimited. (377ABW-2015-0409 dtd 26 May 2015)

13. SUPPLEMENTARY NOTES

14. ABSTRACT
This report details the development at the Space Sciences Laboratory of the University of California, Berkeley of the SupraThermal Electrons, Ions, and Neutrals (AF-STEIN) instrument for the Air Force that can measure essentially all important suprathermal (~4 to 200 keV) particle populations associated with solar disturbances, magnetic storms and magnetospheric substorms. AF-STEIN has several distinct advantages over standard detectors flown on low-earth-orbit (LEO) satellites. AF-STEIN provides the sensitivity, temporal resolution, energy resolution (~1 keV FWHM), dynamic range, and energy range to simplify and improve measurements of suprathermal particle populations in LEO. Typical charged particle Silicon detectors have energy thresholds of ~20keV as opposed to the 2-4 keV threshold developed here. Unlike an electrostatic analyzer which measures one energy band and species at a time, AF-STEIN observes all energies simultaneously and with far higher sensitivity as well as charge state sorting up to several tens of keV.

15. SUBJECT TERMS
Space Particle, Sensor, Electrostatic Analyzer, Suprathermal

16. SECURITY CLASSIFICATION OF:			17. LIMITATION OF ABSTRACT	18. NUMBER OF PAGES	19a. NAME OF RESPONSIBLE PERSON Adrian Wheelock
a. REPORT Unclassified	b. ABSTRACT Unclassified	c. THIS PAGE Unclassified	Unlimited	26	19b. TELEPHONE NUMBER *(include area code)*

Standard Form 298 (Rev. 8-98)
Prescribed by ANSI Std. Z39.18

This page is intentionally left blank.

Table of Contents

List of Figures

List of Tables

1. INTRODUCTION

This report details the development at the Space Sciences Laboratory of the University of California, Berkeley (UCB/SSL) of the SupraThermal Electrons, Ions, and Neutrals (AF-STEIN) instrument for the Air Force that can measure essentially all important suprathermal (~4 to 200 keV) particle populations associated with solar disturbances, magnetic storms and magnetospheric substorms. AF-STEIN has several distinct advantages over standard detectors flown on low-earth-orbit (LEO) satellites. AF-STEIN provides the sensitivity, temporal resolution, energy resolution (~1 keV FWHM), dynamic range, and energy range to simplify and improve measurements of suprathermal particle populations in LEO. Typical charged particle Silicon detectors have energy thresholds of ~20keV as opposed to the 2-4 keV threshold developed here. Unlike an electrostatic analyzer (ESA) which measures one energy band and species at a time, AF-STEIN observes all energies simultaneously and with far higher sensitivity as well as charge state sorting up to several tens of keV.

2. BACKGROUND

For the STE instrument on NASA's STEREO mission UCB/SSL developed silicon semiconductor detectors (SSDs) capable of measuring suprathermal particles down to ~2 keV, covering energies below ~30 keV that are typically measured by electrostatic analyzers (ESAs). AF-STEIN utilizes these SSDs to cover the essential energy range from a few to ~10keV that contributes to spacecraft charging and atmospheric heating by auroral electrons, as well as the ~100keV electrons which penetrate to the lower edge of the ionosphere and can cause significant changes to atmospheric ozone chemistry [1]. AF-STEIN can easily map the boundaries of the auroral zone, continuing and refining the work of the DMSP-Space Environment Sensors, but in a smaller package, with lower mass, and requiring less power. AF-STEIN can obtain definitive measurements of the low energy part of the poorly understood relativistic electron microbursts - short (~0.1s) bursts of electrons from 10s of keV to >1MeV that have been shown to be essential in quantifying the source and loss of relativistic electrons in the radiation belts [2]. Low energy microbursts are a signature of the dynamics of the radiation belt and observations of these particles can even be used as a proxy for understanding the acceleration of high-energy electrons that can have damaging effects in the radiation belt during magnetic storms [3]. Microbursts have small spatial structures [4] and these may contribute to day and nightside ionospheric irregularities which affect radio signal propagation. Rocket measurements suggest that microburst electrons may be limited to energies above the ~20 keV [5], but impulsive microburst-like electron precipitation with energies of a few keV has been detected by ESA instruments on FAST (C. Carlson, private communication). AF-STEIN covers from ~4 keV to ~200 keV with a single detector, and thus will be able to determine unambiguously the relationship of keV energy microbursts to higher energy microbursts. It will measure the full ~4-200 keV spectrum of the intense ion precipitation observed by FAST ESAs only up to ~20 keV (Fig. 1), crucial for obtaining the total deposited energy. Note in figure 1 that dynamic ranges (vertical color bars on right side) assume a 10keV wide band for determining maximum and minimum fluxes.

Some elements of STEIN were designed with the intended goal of flying the detector on a cubesat or a series of cubesats. The CINEMA (Cubesat for Ions Neutrals Electrons and Magnetic

fields) was the primary intended host for STEIN. Additionally some calibration efforts were performed with the CINEMA spacecraft as an element of the readout. This resulted in some lower resolution calibration data than STEIN naturally generates. Because AF-STEIN may not fly on that particular satellite, it may be necessary at some point to make small changes to the programming of the STEIN digital electronics. This is easily accomplished with minor disassembly to access the FPGA programming connector, and the flexibility in doing so is a significant attribute of the STEIN system, however care should be exercised in doing so.
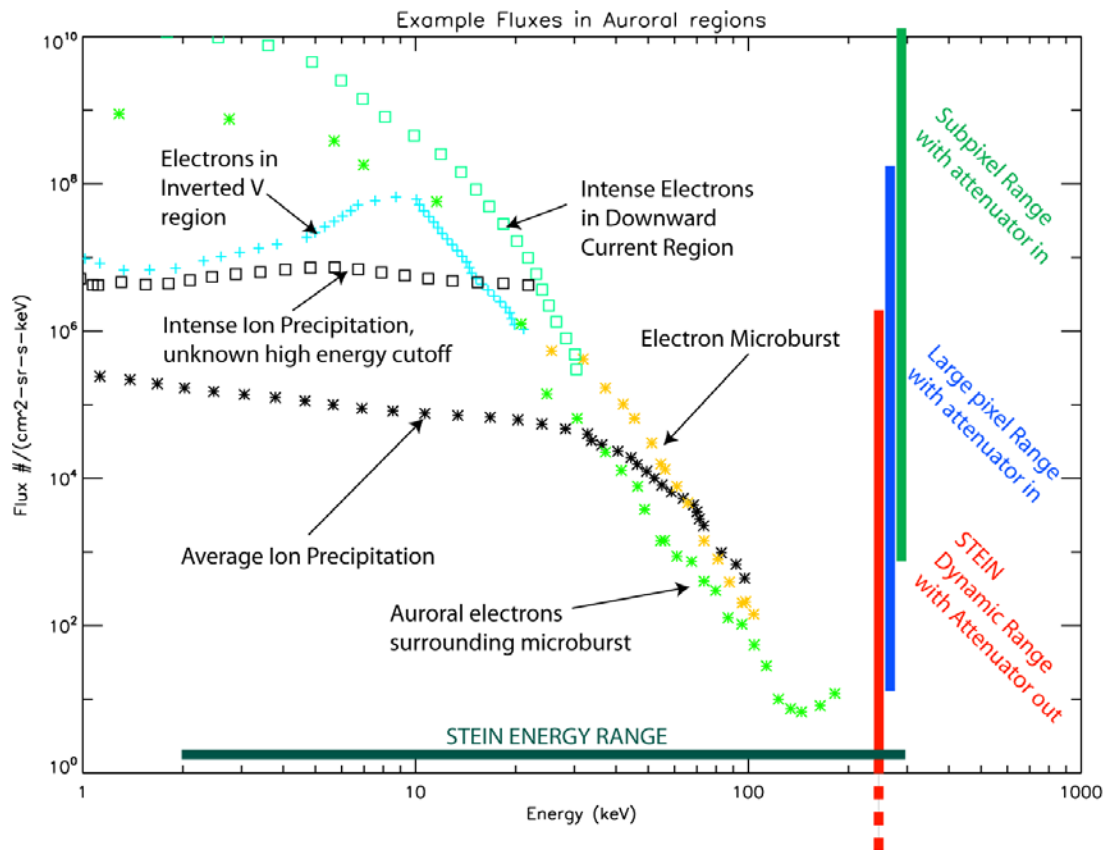

Figure 1. Auroral Fluxes and STEIN's Operating Ranges.

3. METHODS, ASSUMPTIONS, AND PROCEDURES

Description of the STEIN instrument

STEIN begins with a thin window, high resistivity Silicon which allows for penetration of lower energy electrons and ions [6]. Energy loss of electrons in the window is ~350eV and protons lose ~2 keV. These combined with electronics thresholds set the minimum energy particles that can be observed. The completed wafer used to fabricate STEIN is shown in figure 2. The pixelated back contact side is shown
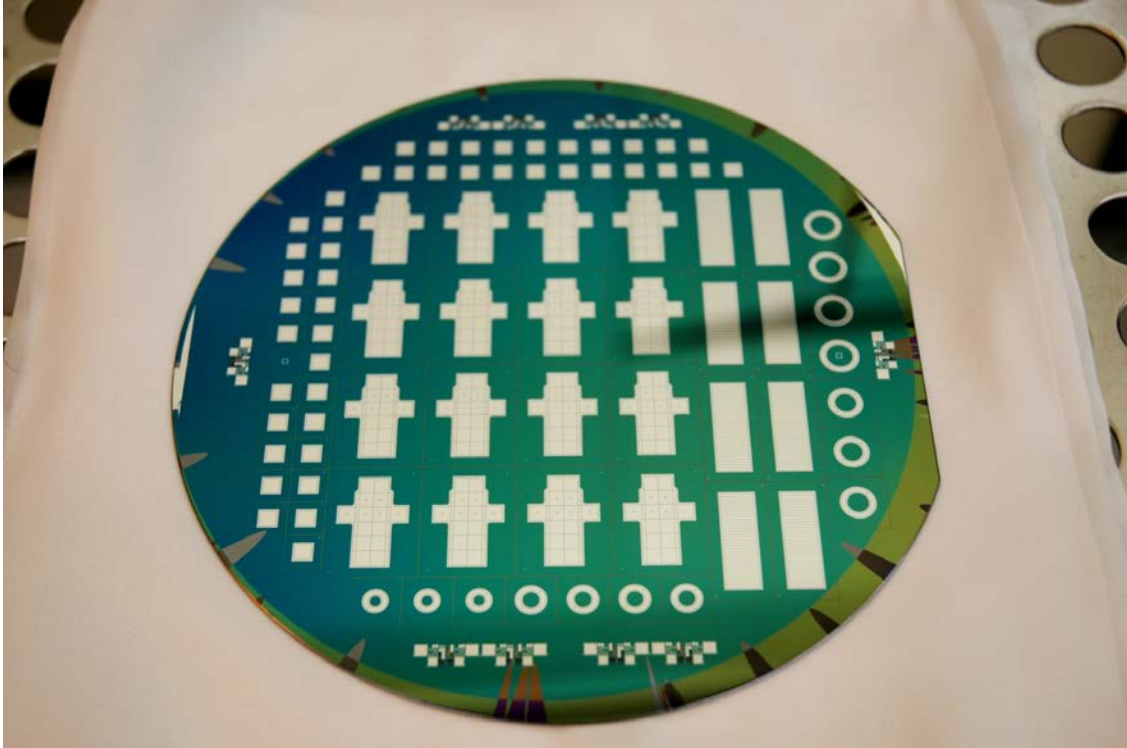

Figure 2. The Completed STEIN Wafer.

Complete depletion of the detector is achieved at >30V and leakage currents range from 100-300pA/cm^2 across the range of 30V to 100V applied bias voltage. The detector's thin windows (opposite side to the pixelated contact side shown in figure 1) are coated with 200 Angstroms of Aluminum/1% Silicon. This reduces the light sensitivity below the level that caused issues on STEREO. Direct viewing of the sun is expected to saturate the detector, however earthshine and moonshine and moderate lab illumination are acceptable levels of illumination. In practice these moderate illuminations increase the leakage current in the detector which raises the low energy threshold and reduces the energy resolution. Figure 3 shows the expected transmission of the coating.
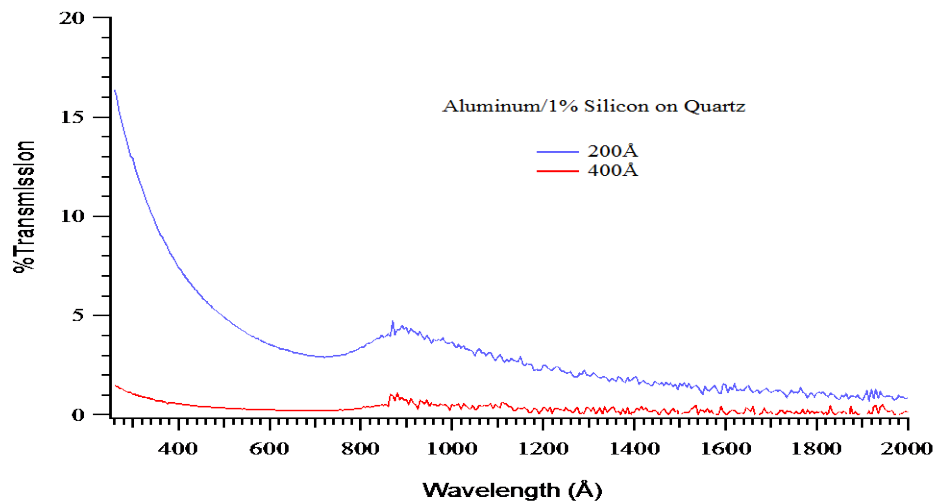
Figure 3. Transmission Through STEIN Coating.

The backside of the detector is pixelated into 30 pixels on one chip in a cross shape as well as two stand-alone pixels which serve as background monitors. A pixel map which is to scale except for pixels 0 and 31 (the background pixels) is shown in figure 4. Units on the figure are 500 um for each tick mark.
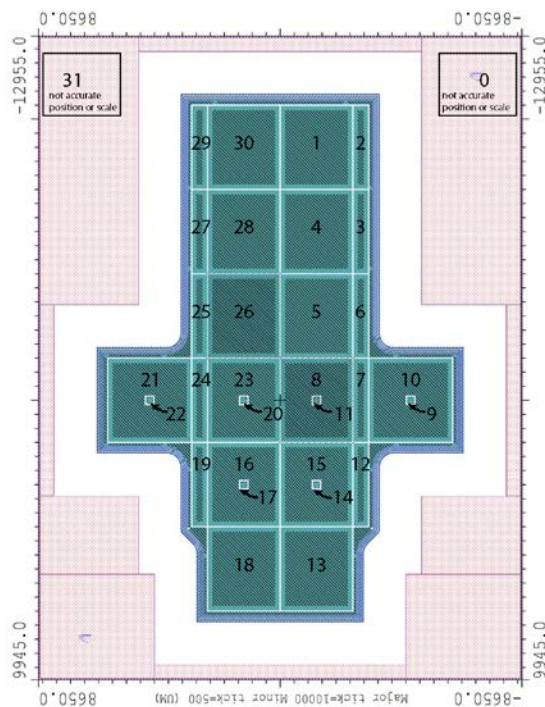

Figure 4. The STEIN Pixel Map.

STEIN electronics:
The output of the Silicon detector just described is connected to a 32 pixel IDeF-X ASIC provided by colleagues at CEA in Saclay, France. The ASIC is as described in [7], although the ASIC was originally designed for the opposite polarity of operation it can be configured to cathode connection as we are using it in STEIN. The detector and ASIC board are mounted on a small board that is mounted in a shield. The ASIC is positioned as close as possible to the detector to minimize capacitance on each channel. The second board is an analog board with an A/D converter and analog processing. It also contains a calibrator circuit that can be used with the ASIC to test the low energy part of the gain in flight. It also has two two-channel DACs for control of sweep voltages, detector bias voltage and calibrator level. Finally a third digital board contains an Actel FPGA for control of the analog electronics, including an overcurrent monitor and communication with the host spacecraft electronics. A block diagram of the three boards is included as figure 5. Schematics for the three boards are available from UCB-SSL[8].

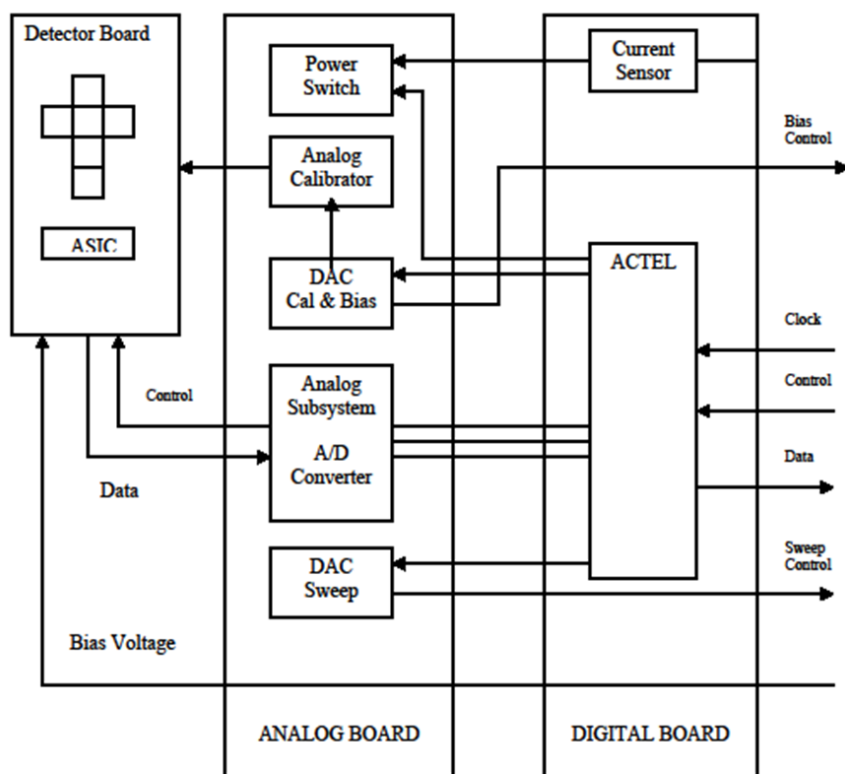**Figure 5. STEIN Electronics Block Diagram.**

The 3 electronics boards are closely stacked as shown in figure 6. The STEIN ASIC is shown under microscope in Figure 7, and the analog board showing the pixelated side and its wire bond attachment scheme is shown in closeup in figure 8. Clearly visible in this image is the use of a high resistivity board material, Rogers 4003, with soft bondable gold pads.
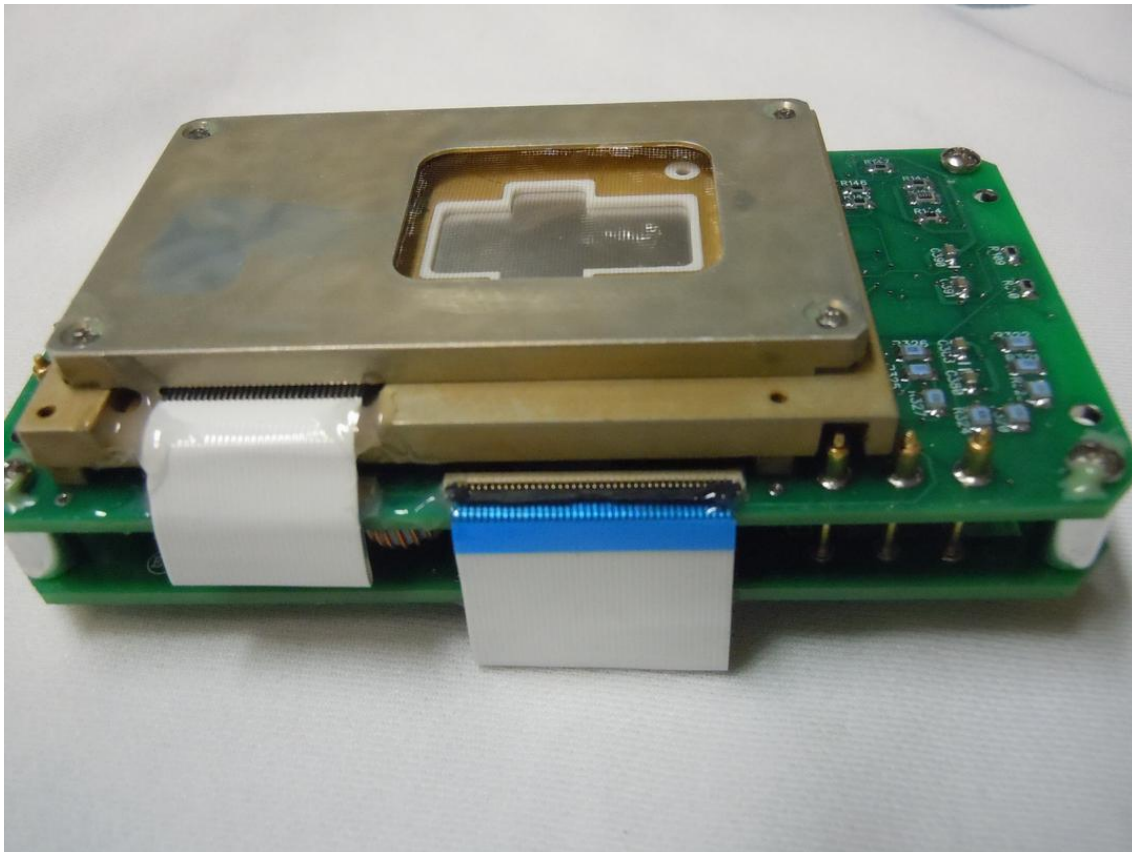
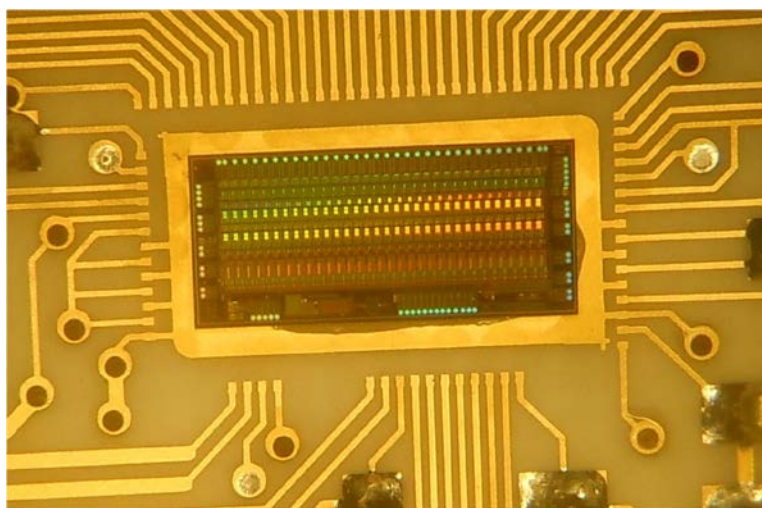**Figure 6. The STEIN Detector and Electronics.**

Figure 7. The IDef-X ASIC as Mounted in STEIN.

Figure 8. The STEIN Detector Board.

The STEIN digital process is handled by an ACTEL IGLOO FPGA. The FPGA controls the ADC and DACs on the subsequent board, does some power switching and watches for an overcurrent from the analog boards, sets on ASIC registers (threshold, peaking time, anode vs. cathode, compensation currents etc.), and responds to triggers from the ASIC. Each pixel can set its threshold individually using 6 bits of registers from ~-2keV to 23keV or by setting the threshold to 63 (the maximum 6 bit value) the pixel can be turned off entirely. This functionality allows the dynamic range in counting of STEIN and prevents the instrument from being saturated with noise counts if any pixel becomes excessively noisy or if the observation goals do not require a certain type of pixel from the pixel map.

When a pixel hit occurs the ASIC will report all pixels with coincident energy deposition. Reading out the map of the triggered pixels takes 32 clock cycles followed by analog readout of the pixel voltage this ends up being a contribution to instrument deadtime in any case where large numbers of single triggers are occurring. During much of our testing we found that most triggers were single triggers, however in high flux situations this will not be the case. STEIN sets the ASIC to a default of 6 microsecond shaping time. The total deadtime for a single hit readout is, at the default settings, ~10us. At these default settings, the STEIN ASIC produces about 25 mv/fC of charge collected from the detector. The analog voltages are passed out serially to the ADC for conversion.

The STEIN FPGA is designed to accept a clock from its host spacecraft (as was the design case for CINEMA) of 8.38MHz (specifically 2^{23} Hz). As well as a spacecraft synced clock at 2Hz. The FPGA currently forms an event record for every event registered by the ASIC. The event record consists of the pixel ID, an 8 bit time tag relative to the 2 Hz clock which provides 1/512 second resolution, and 16 bits of energy information from the ADC. The block diagram of FPGA modules is shown in figure 9. The IIB shown in this figure referes to the instrument interface board that was the primary interface for CINEMA. The interface protocol is CDI,

which shares some similarities to SPI and is described in great detail in various Space Science Lab ICDs[8]. The FPGA code is written in VHDL and can be accessed at the web address in reference 9.
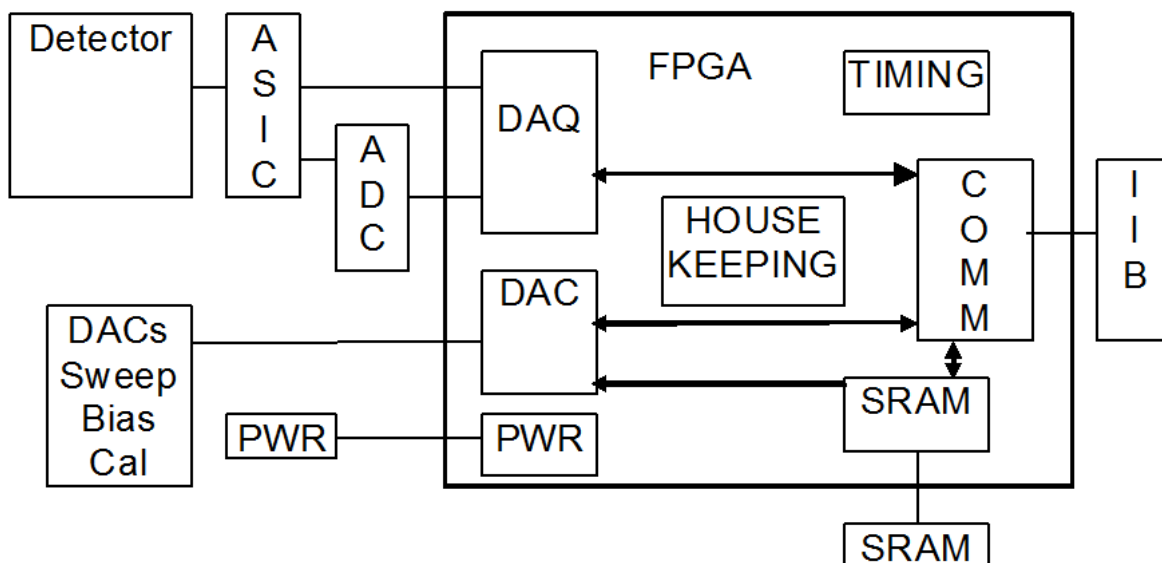

Figure 9. The STEIN FPGA Block Diagram.

The STEIN ASIC outputs pulse height information relative to a "pedestal" value. This pedestal is not expected to be constant with temperature, mission life, or other unknown factors. However, all ground testing indicates that it is a slow function of time. To resolve this unknown and determine an actual energy deposition, the FPGA can set a test pulser on the analog board to inject a known amount of charge to an input capacitor that can be connected to each ASIC channel. This routine needs to be commanded by the spacecraft. An example of the output data for a particular channel is shown in figure 10. The channel gain is determined by fitting these peaks and the pedestal is determined by extrapolating to zero energy. Similar results were obtained when using the test pulser and when using Am-241 spectral lines. The scaling of the Y-axis in the figure only depends on the length of time that the test pulser was set at each value. For reference the values shown represent test pulser levels of 0x19, 0x1E,0x28,0x50, and 0xA0 as the most significant bits used in setting the DAC (0x00 represents the lower bits).

The FPGA also controls DACs that can set the control voltage on the BIAS supply used for CINEMA. This functionality is not required if the Bias voltage is determined elsewhere. Likewise the FPGA is able to output control voltage to a high voltage power supply to modulate the voltage found on the electrostatic deflectors. This "sweep" voltage can be set as a table in the FPGA which is cycled through on a 1 Hz clock. This functionality also does not need to be used if the voltage applied to the deflector plates is controlled elsewhere. It does have the advantage of syncing any cyclical aspect of the sweep voltages with the time tagging of particle counts. The

sweep table can have 1,2,4,8…128 possible steps in each 1s. Memory is available for two sweep tables so that one can be loaded while the other is in use.

An unused DAC is found in the schematics which could in principle be used to subtract the pedestal voltage. Jumpers on the board are in place for this change to be made easily, however the current configuration is to digitally subtract the pedestal on the ground.

When the analog board is off, the power draw is ~200 mW on the 3.3 V and 1.5 V line (3.3V current plus 1.5V current is 100mA). Once its analog components are turned on a typical power draw is around 400mW. At high count rates the power draw increases marginally to around 460mW. When the analog board is on the digital current draw will drop to 70mA on the 3.3 and 1.5V line combined. The STEIN pinout is found below in Table 1.

Table 1. STEIN Pinout

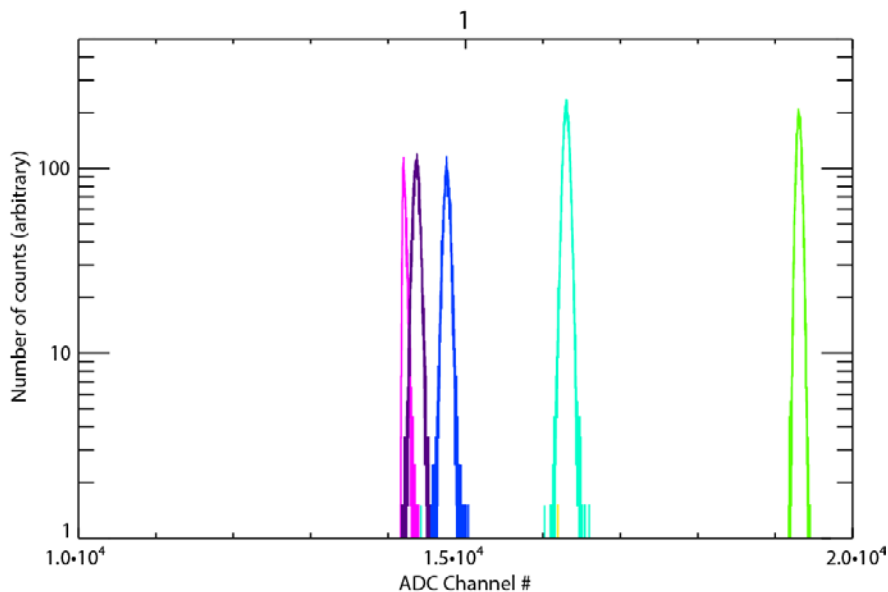| STEIN pinout on 21 pin Airborn MK-232-021-125-2200			
Pin #	Name	Pin #	Name
1	Bias +V (30-50V)	12	N/C
2	Bias Return	13	N/C
3	SDOO	14	SDIN
4	SCKIN	15	SSO
5	1sectic	16	+5VA
6	HVCTL GND	17	-5VA
7	3.3V	18	DGND
8	1.5V	19	DGND
9	AGND	20	AGND
10	BIAS CTL	21	SWEEP1 CTL
11	SWEEP2 CTL		

Figure 10. Channel 1 Responding to 5 Different Test Pulser Inputs.

STEIN weighs approximately 350 grams and at it widest along its long aperture it is 9.5cm in length, along its shorter aperture including the internal attenuator it is 8.6cm. Along the axis of

9

its field of view (FOV) it is 7.5 cm. Solid works and STEP files of all the mechanical parts will be made available at the previously referenced website. A completely assembled STEIN is pictured in Figure 11.
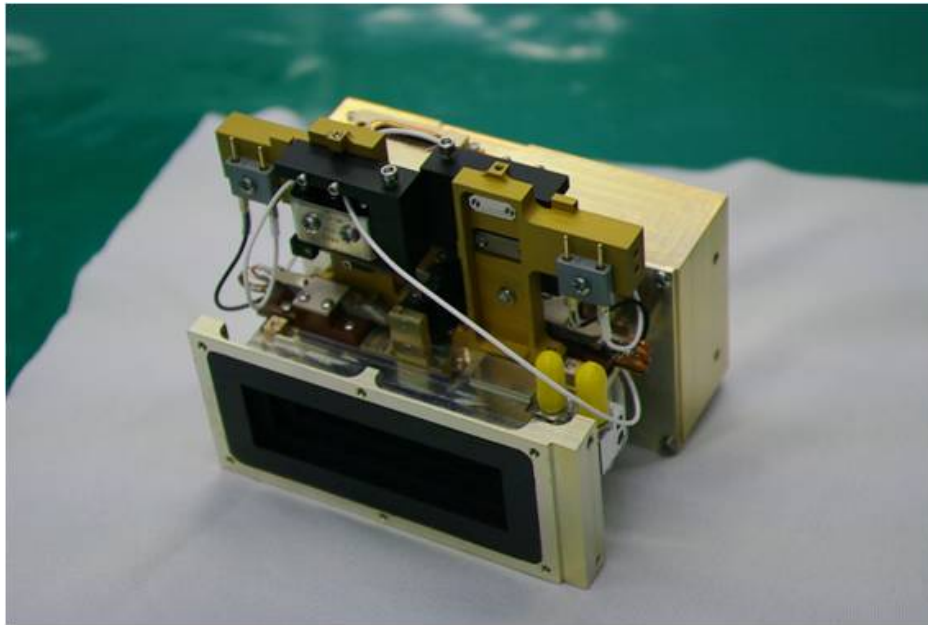

Figure 11. One Copy of the STEIN Instrument.

The front aperture is set by a series of thin photoetched BeCu blades which are blackened with Ebonol C. The BeCu baffles are epoxied into place. For the delivered instrument the frontmost baffle has been omitted because of the uncertainty of its launch. The baffle can be added at any time, or omitted. The remaining 4 baffles do a sufficient job of defining the field of view for low energy particles and adding the final front baffle makes the instrument very delicate with the likely smudging of the ebononl C coating and the possible deposit of that material onto the detector surface. The baffle opening angle along its long axis is 65.4 degrees and the FOV as defined by the deflector plates is 18.8 deg. The baffle opening across its short axis is 40 deg as pictured in Figure 12. With no deflector voltage applied the FOV is determined by the deflector geometry, while when a voltage is applied there is a combination of factors determining the field of view in that plane that involves the applied voltage, the geometry of both the baffles and the deflector, the angle, energy and position of the charged particle. Neutral particle FOVs are always determined by the 18.8 deg. opening angle.

Although often referred to as a deflector plate, the deflector is made up of a series of sandwiched BeCu blades to reduce scattering of incident particles, primarily electrons, into the detector which would confuse the angular response of the instrument for all species. The deflector assemblies are separated by 4mm and can support a voltage differential of +/- 2kV (4kV total) which was verified during thermal vacuum testing of the instrument. One half of the assembly is visible in figure 13. And the assembled deflectors are visible in Figure 14. The left image in Figure 14 has had the baffles removed to show the detector plane more clearly.
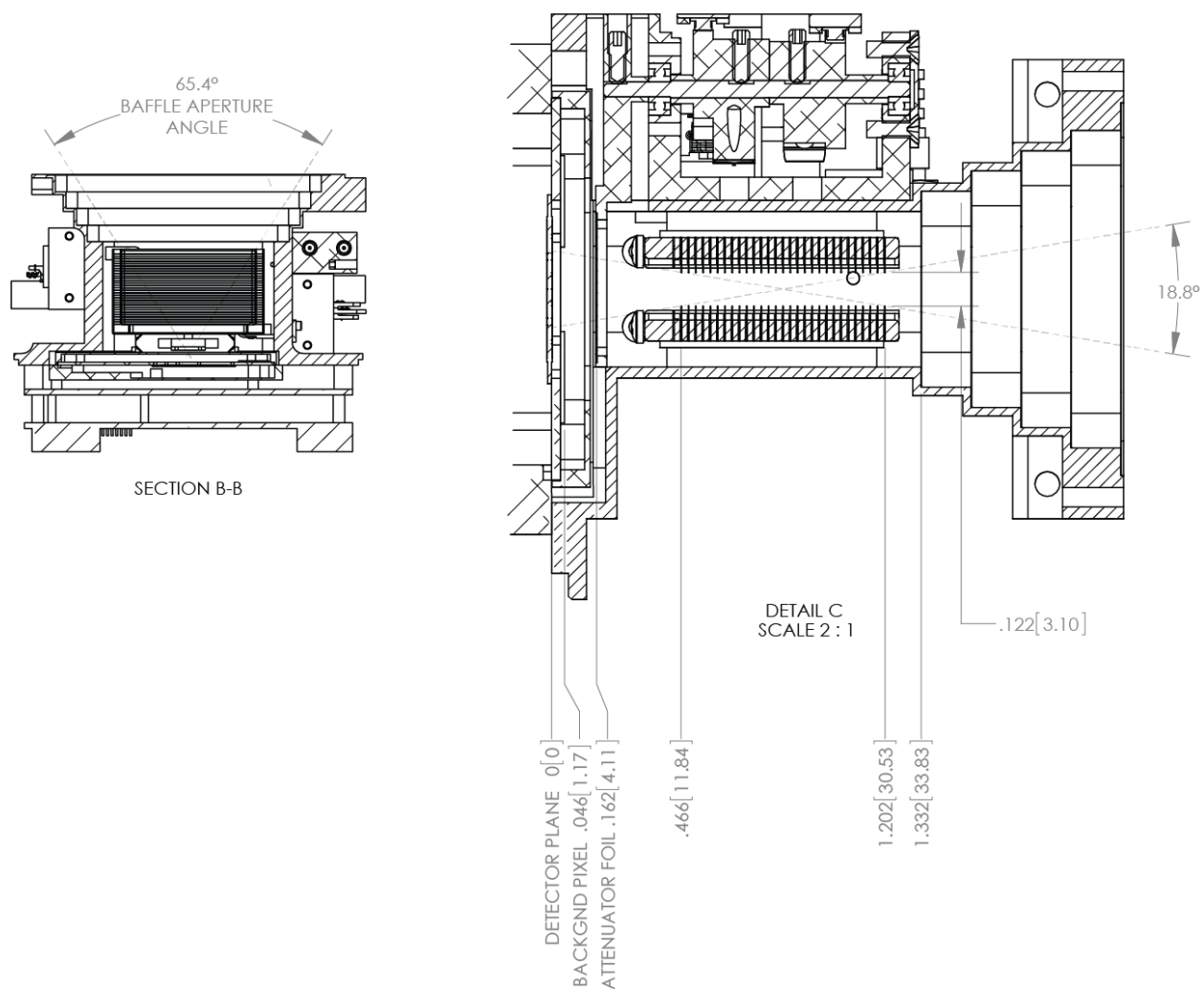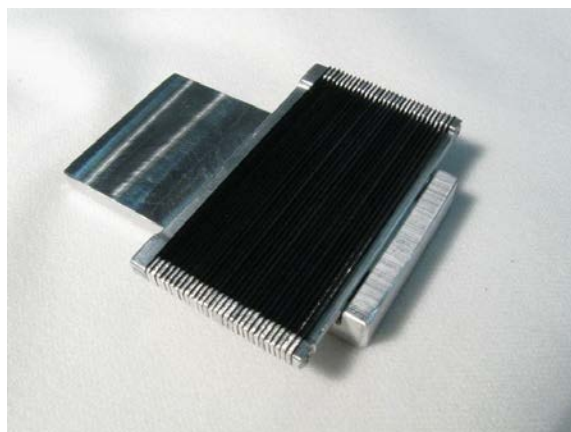
Figure 12. The STEIN FOV Determining Elements.

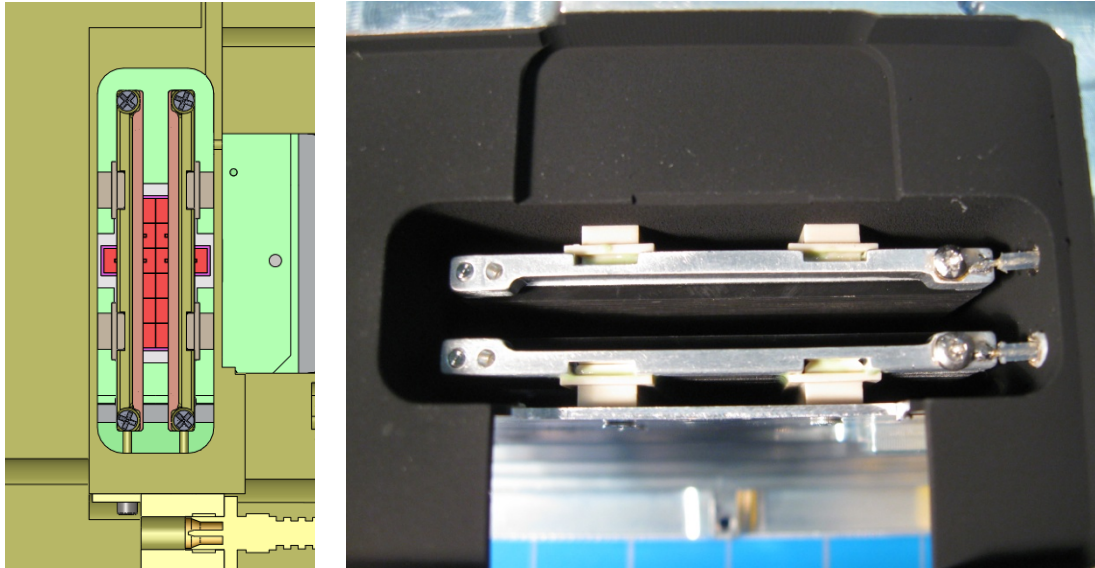**Figure 13. Half of an Assembled Deflector.**

Figure 14. View of the Deflectors.

The Electric field within the aperture has been modeled using the SIMION software and field strengths are similar to an ideal parallel plate are found, with minor fringing fields.The results are shown in Figure 15. The Geant4 simulations that are described later used this field for determination of response. The deflector voltage is connected with a Reynolds HV connector and the connection is found under the yellow covers pictured in Figure 11.
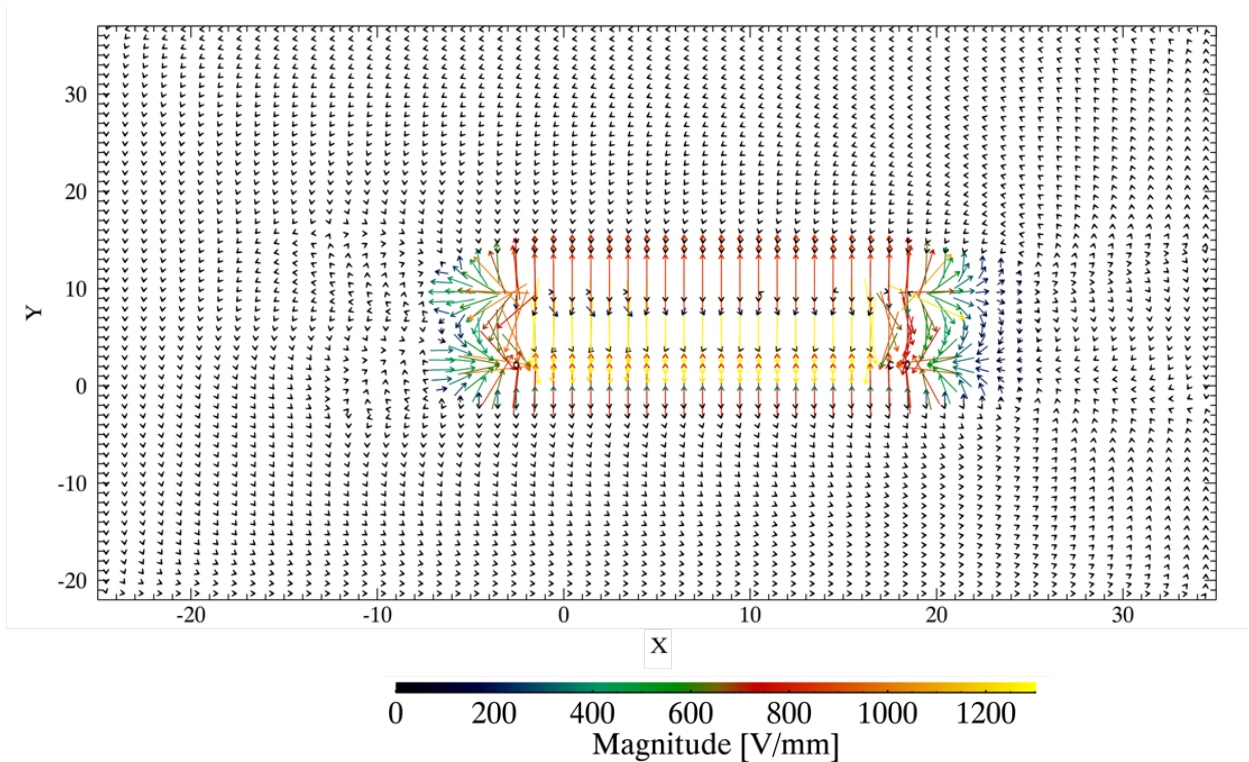

Figure 15. **The Electric Field Inside the STEIN Deflector Region.**

STEIN has a mechanical attenuator that can change the effective area of the particle detector and reduce its counting rate to a manageable range when the instrument is encountering high fluxes of particles. The attenuator is moved into and out of place by a pair of nanomuscles that were tested for CINEMA with an applied current between 580 and 780mA for 0.15 second. Putting the attenuator paddle in the field of view reduces the geometric factor by ~100, although further calibration of this number as a function of energy and angle has not been performed. The attenuator is visible as the top of Figure 11 or below in model form as figure 16. The power applied for both attenuator in and attenuator out come in on separate 2 pin Winchester-type connectors visible in Figure 11.
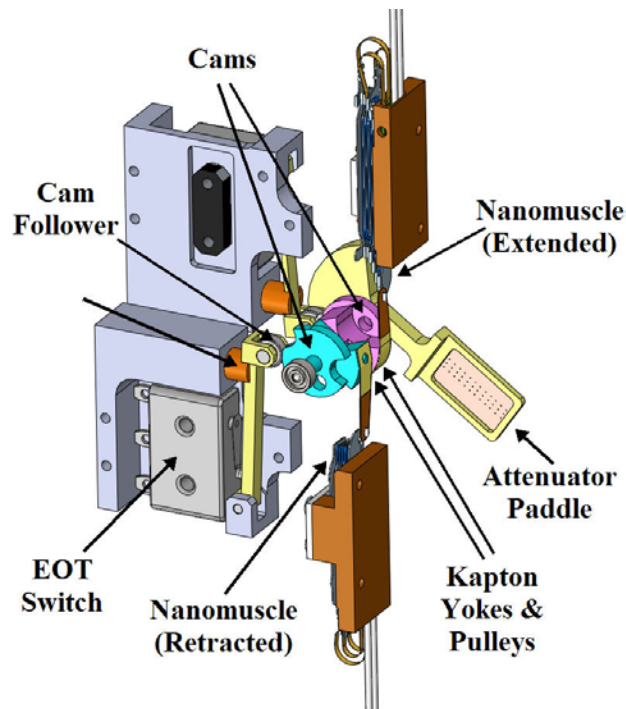

Figure 16. The STEIN Attenuator Assembly.

4. RESULTS AND DISCUSSION

The STEIN instrument has been tested using a number of X-ray and electron sources and the design has been simulated in the Geant4 and SIMION modeling environments. X-ray data and an electron source is shown for a few pixels demonstrating the high energy resolution and low threshold of the instrument. Energetic beam data was taken with the CINEMA electronics readout, so energy resolution is quite poor, but the performance of the instrument can be judged at a basic level. Significantly more calibration data taken in operating conditions for whatever desired final configuration is determined should be conducted. Various calibration data sets and software required to extract useful information from them will be posted to the web archive.

X-ray data from an Am-241 source are shown in 17 for one of the large central pixels. For this test the pixel threshold was set at value 20 which is a nominal cutoff of 7 keV. This was done for expedience, but routine measurement in a quiet environment at threshold 10 is achievable. There is no noticeable increase in the noise at the low energy cutoff.
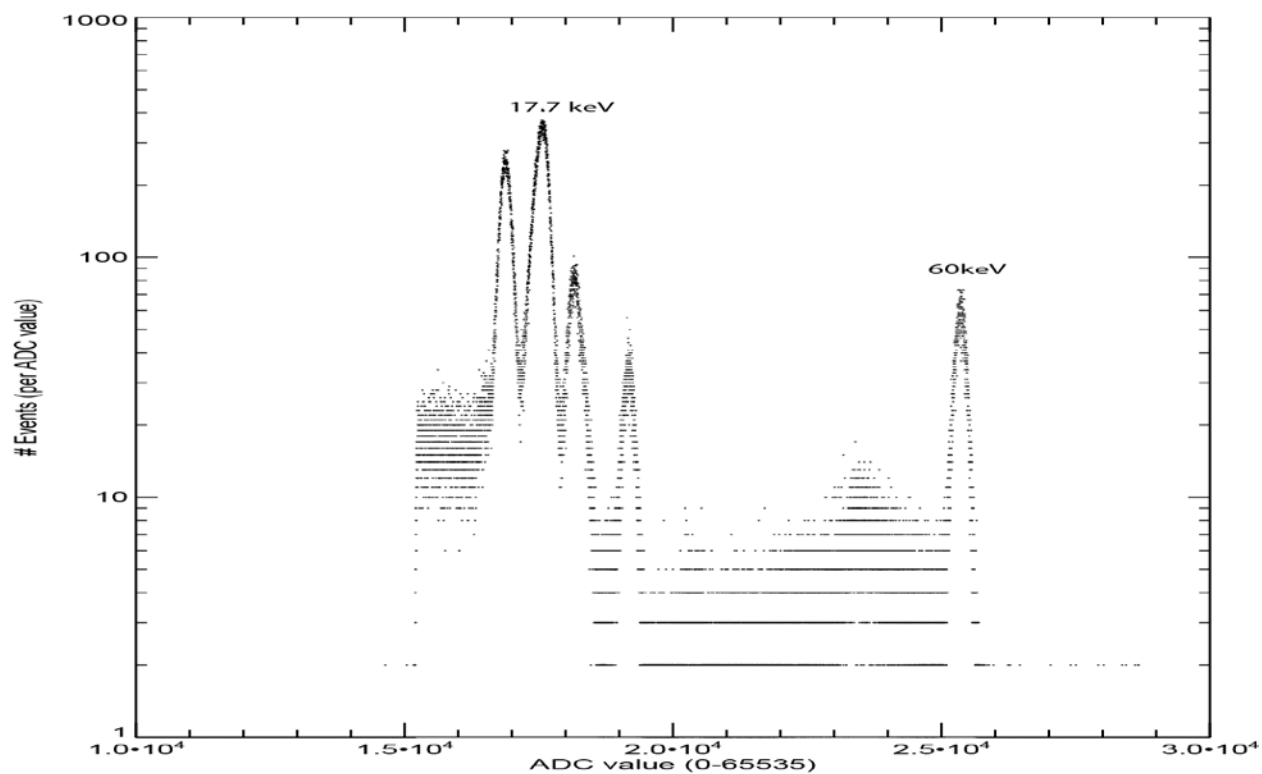
Figure 17. Am-241 Spectrum from STEIN

STEIN was tested in a beam chamber with the CINEMA spacecraft and the results of several of those tests are shown in the following figures. Figure 18. Shows a central pixel with no deflection voltage applied and incident 10,20,30, and 40 keV electrons. The x-axis has crudely been converted to energy because the CINEMA down sampling is so severe. The presence of many scattered electrons obscures the low energy response of the detector. Care must be exercised to determine the contribution of higher energy electrons to the detected energy.
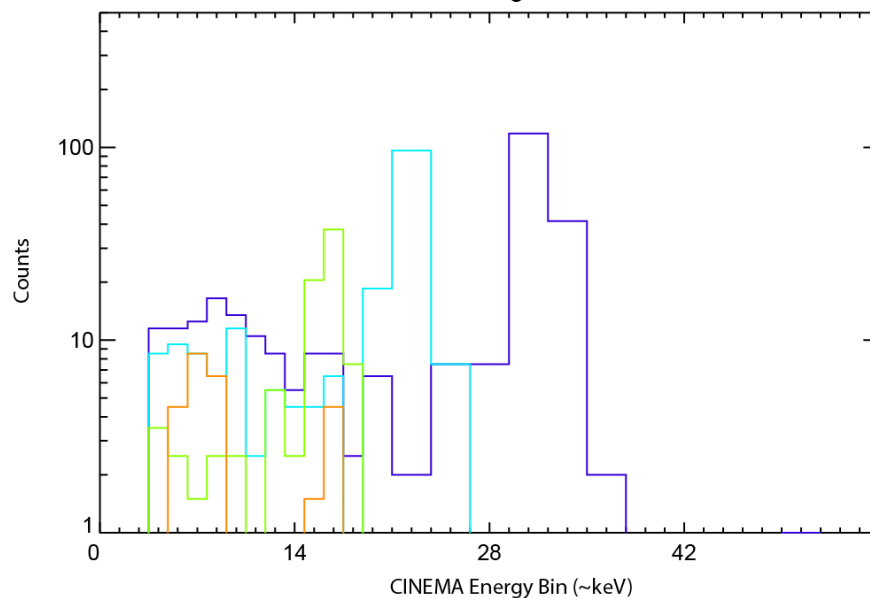

Figure 18. 10,20,30,40 keV Electron Beam Results for STEIN.

Figure 19. shows a pixel on the side of the detector respond to 100 keV protons as deflector voltage is increased from +/-1kV (yellow) to +-2kV (purple). The corresponding pixel on the opposite side of the detector shows no response. X-axis units are CINEMA bins that have not been corrected for gain or pedestal.
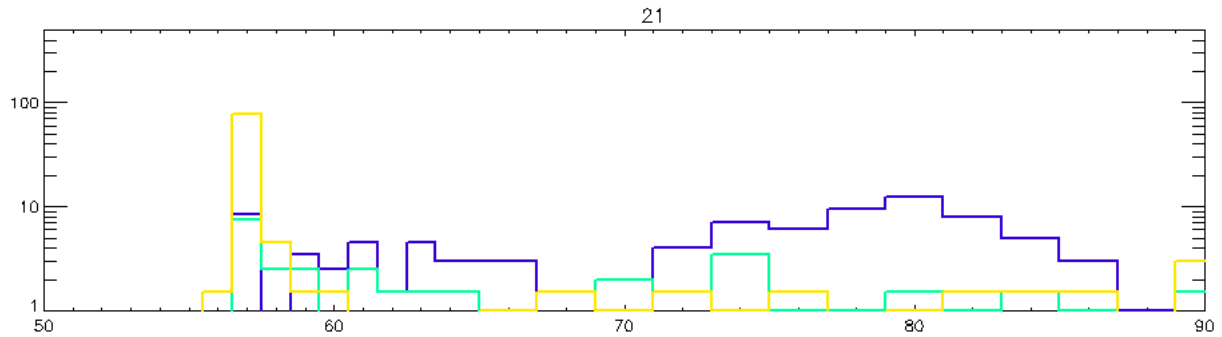

Figure 19. STEIN Pixel Response with Varying Sweep Potential.

Monte Carlo simulations of the detector performance were made using the Geant4 modeling toolkit by converting the SolidWorks CAD files to the geant GDML format. The GDML file is also available for use. A rendering of that model is shown in figure 20.
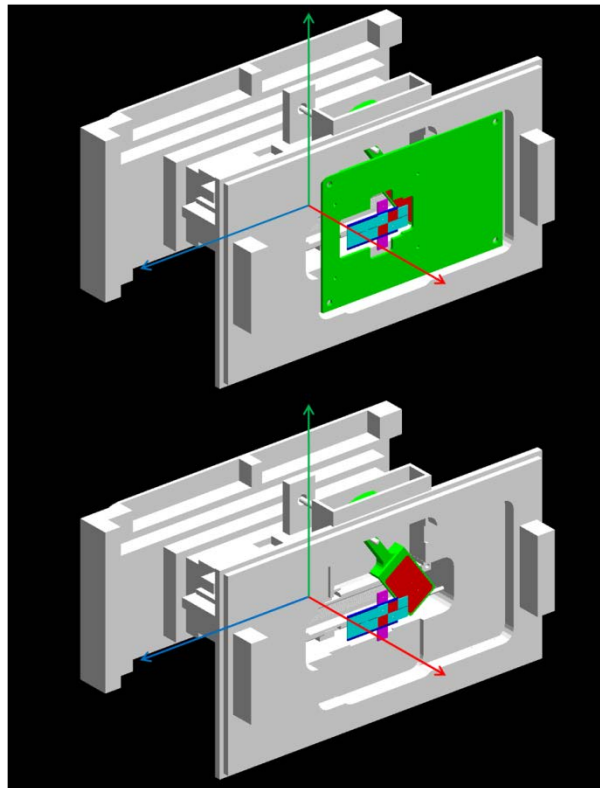

Figure 20. The STEIN GDML Model.

Using the STEIN model it is possible to explore a wide parameter space for instrument operation. The GEANT simulation was used to create a measure of geometric factor as function of energy and pixel at a full +/-2 kV deflection the results of that simulation are shown in Figure

21. At this deflection level, 20keV electrons are almost entirely excluded except for a few scattered hits. At 50keV it is clear that the geometric factor increases by a factor of 3 for equivalent sized pixels on the detector left hand side (low number pixels) as opposed to the right hand side this is a result of the electrostatic field bending electrons rightward towards higher number pixels. At higher energies the electrostatic field does not significantly affect the trajectory of the electrons and 200keV electrons have similar geometric factors on both sides of the instrument.
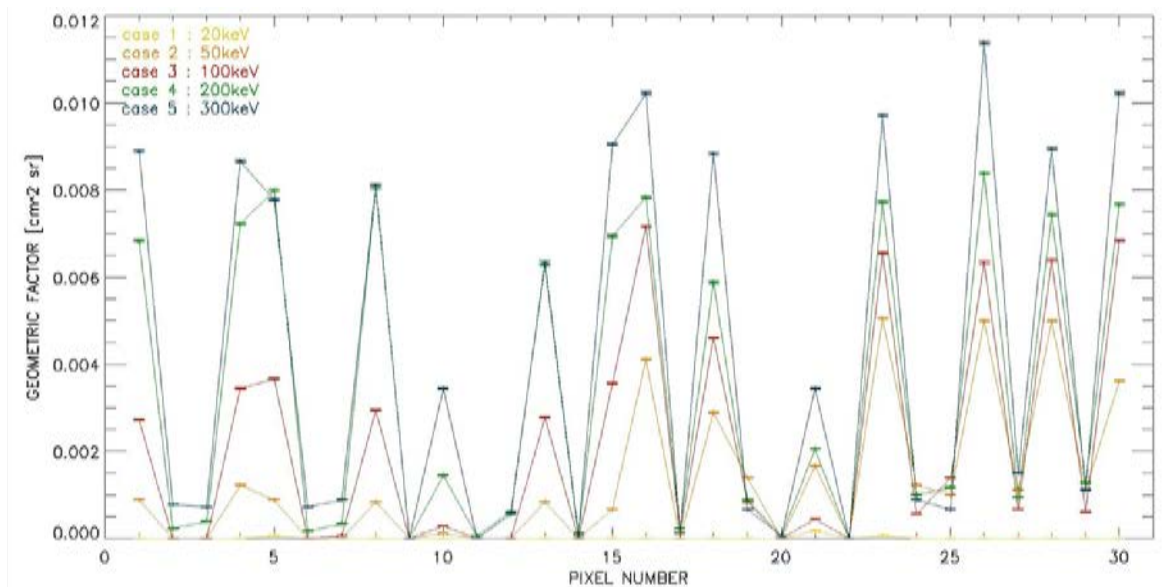

Figure 21. The STEIN Electron Geometric Factor at +/-2kV.

5. CONCLUSIONS

The STEIN instrument is a capable, flexible instrument that requires low mass, power, and volume resources while measuring ions electrons and .neutrals from a few to ~200keV. With an electrostatic deflector it is able to sort most charged and uncharged particles up to ~30keV. Not all electron scattering issues have been resolved, and more calibration data should be taken. Readout of the instrument should occur at better than the 7 bit energy resolution that was planned for CINEMA in order to accurately understand the instrument response. Despite these caveats the versatility and capabilities of STEIN make it a useful instrument to try to put into practical application.

REFERENCES

[1] Randall, C. E., V. L. Harvey, C. S. Singleton, P. F. Bernath, C. D. Boone, and J. U. Kozyra, "Enhanced NOx in 2006 linked to strong upper stratospheric Arctic vortex," *Geophys. Res. Lett.*, 33, L18811, doi:10.1029/2006GL027160.

[2] Lorentzen, K. R., M. D. Looper, and J. B. Blake, "Relativistic electron microbursts during the GEM storms," *Geophys. Res. Lett.*, 28, 2001, pp. 2573-2576.

[3] O'Brien, T. P., K. R. Lorentzen, I. R. Mann, N. P. Meredith, J. B. Blake, J. F. Fennell, M. D. Looper, D. K. Milling, and R. R. Anderson, "Energization of relativistic electrons in the presence of ULF power and MeV microbursts: Evidence for dual ULF and VLF acceleration," *J. Geophys. Res.*, 108(A8), 1329, doi:10.1029/2002JA009784.

[4] Blake, J. B., M. D. Looper, D. N. Baker, R. Nakamura, B Klecker, and D. Hovestadt, "New high temporal and spatial measurements by SAMPEX of the precipitation of relativistic electrons," *Adv. Space Res.*, 18(8), 1996, p. 171.

[5] Datta, S., R. M. Skoug, M. P. McCarthy, and G. K. Parks, "Analysis and modeling of microburst precipitation," *Geophys. Res. Lett.*, 23(14), 1996, pp. 1729-1732.

[6] C.S. Tindall, N.P. Palaio, B.A. Ludewigt, S.E. Holland, D.E. Larson, D.W. Curtis, S.E. McBride, T. Moreau, R.P. Lin, V. Angelopoulos, "Silicon detectors for low energy particle detection," *Trans. Nucl. Sci.,* 2008.

[7] Gevin, O.; Baron, P.; Coppolani, X.; Daly, F.; Delagnes, E.; Limousin, O.; Lugiez, F.; Meuris, A.; Pinsard, F.; Renaud, D., "IDeF-X ECLAIRs: A CMOS ASIC for the Readout of CdTe and CdZnTe Detectors for High Resolution Spectroscopy," *Nuclear Science, IEEE Tran,* 10.1109/TNS.2009.2023989, 2009, pp. 2351-2359.

[8] An archive of relevant binary files and data, http://sprg.ssl.berkeley.edu/~jsample/afrl, last modified February 27, 2015, Accessed February 27, 2015.

List of Symbols, Abbreviations, and Acronyms

ADC   Analog to Digital Converter

AFRL   Air Force Research Laboratory

AFSPC   Air Force Space Command

ASIC   Application Specific Integrated Circuit

CINEMA   Cubesat for Ions Neutrals Electrons and MAgnetic fields

DAC   Digital to Analog Converter

DMSP   Defense Meteorological Satellite Program

ESA   ElectroStatic Analyzer

FOV   Filed Of View

FPGA   Field Programmable Gate Array

GDML   GEANT Dynamic Markup Language

GEANT   Geometry ANd Tracking

ICD   Interface Control Document

SSL   Space Sciences Laboratory

STEIN   Supra Thermal Electrons Ion and Neutrals

UCB   University of California, Berkeley

VHDL   VHSIC Hardware Description Language

DISTRIBUTION LIST

DTIC/OCP
8725 John J. Kingman Rd, Suite 0944
Ft Belvoir, VA 22060-6218   1 cy

AFRL/RVIL
Kirtland AFB, NM 87117-5776   2 cys

Official Record Copy
AFRL/RVBXR/Adrian Wheelock   1 cy

This page is intentionally left blank.